

Non-equilibrium wetting transition in a magnetic Eden model

J. Candia^a and E.V. Albano^b

Instituto de Investigaciones Fisicoquímicas Teóricas y Aplicadas, (INIFTA), CONICET, UNLP, CIC (Bs. As.). Sucursal 4, Casilla de Correo 16, (1900) La Plata, Argentina

Received 27 March 2000

Abstract. Magnetic Eden clusters (Ausloos *et al.*, Europhys. Lett. **24**, 629 (1993)) with ferromagnetic interaction between nearest-neighbor spins are grown in a confined 2d-geometry with short range magnetic fields acting on the surfaces. The change of the growing interface curvature driven by the field and the temperature is identified as a non-equilibrium wetting transition and the corresponding phase diagram is evaluated.

PACS. 75.70.-i Magnetic films and multilayers – 05.70.Np Interface and surface thermodynamics – 68.45.Gd Wetting

1 Introduction

The study of irreversible growth models is a subject that has attracted growing attention during the last decades. Nowadays, this interdisciplinary field has experienced a rapid progress due to both, their interest in many sub-fields of physics, chemistry and biology, as well as by their relevance in numerous technological applications. Recent progress in our understanding of growth phenomena, with special emphasis on the properties of rough interfaces, has been extensively reviewed [1–5]. On the other hand, the interaction of a bulk phase of a system with a wall or a substrate may result in the occurrence of very interesting wetting phenomena. Wetting transitions have been experimentally observed and theoretically studied in a great variety of systems in thermal equilibrium, for reviews see *e.g.* [6, 7]. In contrast, the study of wetting phenomena under non-equilibrium conditions has, so far, received much less attention. Within this context, very recently Hinrichsen *et al.* [8] have introduced a non-equilibrium growth model of a one-dimensional interface interacting with a substrate. The interface evolves *via* adsorption-desorption processes which depart from detailed balance. Changing the relative rates of these processes, a transition from a binding to a non-binding phase is reported [8]. In fact, in the study of wetting phenomena under equilibrium conditions, wetting transitions are usually associated to the onset of unbinding of an interface from a wall [9]. The aim of this work is to study the properties of a non-equilibrium wetting transition which takes place in a variant of the irreversible Eden growth model [10], where the

particles are replaced by spins which may adopt two different orientations. Such model is known as the magnetic Eden model (MEM) and has been proposed by Ausloos *et al.* [11]. The MEM has originally been motivated by the study of the structural properties of magnetically textured materials [11]. In the present work, the growing system is confined between two parallel walls where short range boundary magnetic fields interact with the spins. Our investigation of the properties of the MEM in such stripped geometry is also motivated by recent experiments where the growth of quasi-one-dimensional strips of Fe on a Cu(111) vicinal surface has been studied [12]. Also, in a related context, the study of the growth of metallic multilayers have shown a rich variety of new physical phenomena. Particularly, the growth of magnetic layers of Ni and Co separated by a Cu spacer layer has recently been studied [13]. In this case, the interaction between magnetic atoms in the bulk of the respective layer may be different than that of such atoms at the surface in contact with the Cu layer. Such interaction may, in principle, be modeled by introducing a short range boundary magnetic field, as we have proposed in the present work.

2 The model and the Monte Carlo simulation method

In the classical Eden model [10] on the square lattice, the growth process starts by adding particles at the immediate neighborhood (the perimeter) of a seed particle. Subsequently, particles are stucked at random to perimeter sites leading to the formation of compact clusters with a self-affine interface [2–4]. The magnetic Eden model (MEM) [11] considers an additional degree of freedom due to the spin of the growing particles. While early studies

^a *Present and Permanent address:* Departamento de Física, Facultad de Ciencias Exactas, Universidad Nacional de La Plata, C.C.67, (1900) La Plata, Argentina

^b e-mail: ealbano@inifta.unlp.edu.ar

of the MEM have been performed using a single seed placed at the center of the sample [11], for the purposes of the present work we have adopted a different geometry. In fact, we have studied the MEM on the square lattice in a rectangular (or stripped) geometry of $L \times M$ ($1 \leq i \leq M$, $1 \leq j \leq L$) with $L \ll M$. The seed is a column of L spins located at $i = 1$ and cluster growth takes place in one direction only, say for $i \geq 2$. Open boundary conditions are also considered. A surface magnetic field H , acting on the sites placed at $j = 1$ and $j = L$, accounts for the interaction between the walls and the spins. It is assumed that each spin S_{ij} may adopt two possible orientations, namely up and down (*i.e.*, $S_{ij} = \pm 1$). Clusters are grown by selectively adding spins at perimeter sites, which are defined as the nearest-neighbor (NN) empty sites of the already occupied ones. Considering a ferromagnetic interaction of strength $J > 0$ between NN spins, the energy E of a given configuration of spins is taken to be

$$E = -(J/2) \sum_{\langle ij, i'j' \rangle} S_{ij} S_{i'j'} - H \sum_{\langle i, S \rangle} (S_{i1} + S_{iL}), \quad (1)$$

where $\langle ij, i'j' \rangle$ means that the summation in the first term is taken over occupied NN sites and $\langle i, S \rangle$ denotes that the second summation has to be taken over occupied sites on both surfaces. Thus, measuring the absolute temperature in units of J (the Boltzmann constant is set to unity), and the energy and the surface magnetic field in units of J , the change of energy ΔE involved in the addition of a spin S_{ij} to the system is given by

$$\Delta E/T = -(1/T) S_{ij} \sum_{\langle ij, i'j' \rangle} S_{i'j'} - (H/T) (S_{ij} \delta_{j1} + S_{ij} \delta_{jL}), \quad (2)$$

where the summation $\langle ij, i'j' \rangle$ is taken over occupied NN sites keeping i, j fixed, and δ_{j1} and δ_{jL} are standard Kronecker delta symbols. Therefore, the probability of a perimeter site to be occupied by a spin S_{ij} is proportional to the Boltzmann factor $\exp(-\Delta E/T)$, where ΔE is given by equation (2). At each step, all perimeter sites are considered and the probabilities of adding up and down spins have to be evaluated. After proper normalization of the probabilities the growing site and the orientation of the spin are determined through a pseudo-random number generator. It is worth mentioning that while both the Hamiltonian and the Boltzmann probability distribution considered for the MEM are the same as the ones used for the Ising model in a rectangular geometry with surface magnetic fields [9, 14], there exists an essential difference between both models: namely, while the Ising model deals with reversible spin configurations in thermodynamic equilibrium, the MEM corresponds to a far-from-equilibrium irreversible growth model. Therefore, once the bulk of the aggregate is filled it becomes frozen (*i.e.*, it can not be modified any more due to further addition of spins). This property allowed us to use a very well-known efficient simulation algorithm which periodically removes the frozen part of the aggregate and only

keeps track of the active growing interface. In this way one saves computer memory and large aggregates can be studied. In the present work we have used strips of widths $L = 32$ and $L = 64$, and lengths as large as $M = 3 \times 10^7$, generating spin aggregates of up to 10^9 particles. In order to quantitatively characterize the behavior of the system we have measured the average magnetization of the frozen columns, given by

$$m(i, L, T, H) = (1/L) \sum_{j=1}^L S_{ij}, \quad (3)$$

which plays the role of an order parameter. Also, the probability distribution of the order parameter $P_L(m, T, H)$ has been evaluated [15].

3 Results and discussion

It is worth mentioning that we have restricted ourselves to the $H \geq 0$ case without losing generality. In fact, first we have checked that the magnetic Eden growth process in a confined geometry is characterized by an initial transient followed by a non-equilibrium stationary state that is independent from the starting seed. So, we have particularly employed an initial seed entirely constituted by up spins throughout. Thus, changing the sign of the applied field ($H \rightarrow -H$) corresponds to invert spin orientation at every lattice site. Then, the order parameter probability distribution can be simply obtained by replacing $P_L(m) \rightarrow P_L(-m)$. Analogous replacements also hold for other observables that can be computed from $P_L(m)$, such as the average of the absolute column magnetization defined below (see Eq. (4)).

Figure 1 shows typical plots of the probability distribution of the order parameter, as obtained for different temperatures and fields (unless otherwise stated, we consider the case of strip width $L = 32$ throughout).

Since the surface field is always assumed to be positive, all distributions are biased towards positive values of m . Figure 1a shows a typical low-temperature distribution that corresponds to $T = 0.5$. There one observes that for weak fields two peaks of $P_L(m)$ clearly emerge at $m = \pm 1$. Particularly, for $H = 0$ the distribution is symmetric and the average magnetization vanishes. As naturally expected, for $H > 0$ the peak at $m = 1$ is higher due to the applied surface fields. This result points out that the system undergoes fluctuations, since spin columns happen to be mainly builded up by parallel-aligned spins with a single orientation, either up or down. Increasing the field ($H \geq 0.75$) the negative peak of $P_L(m)$ vanishes showing that the surface field is strong enough in order to suppress such fluctuations. At $T = 0.8$ (Fig. 1b), $P_L(m)$ is strongly biased by the field and only small peaks at $m = -1$ can be observed for very weak fields ($H < 0.25$). It should also be noted that the curvature of $P_L(m)$ changes, as compared to Figure 1a. In fact, at $T = 0.8$ and for weak fields

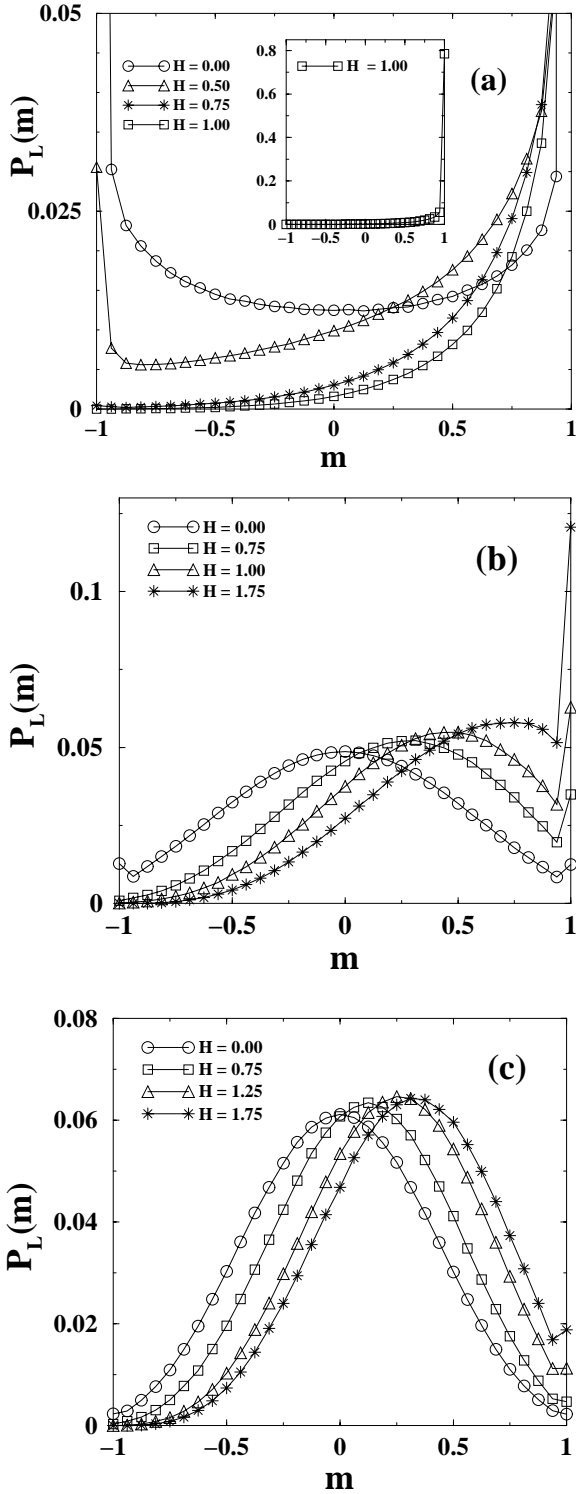


Fig. 1. Plots of the order parameter distribution function $P_L(m)$ versus m obtained for different values of H as indicated in the figures. (a) Results for $T = 0.5$. The vertical axis has been truncated in order to allow a detailed observation of the dependence of $P_L(m)$ with m . The inset shows a plot of $P_L(m)$ versus m obtained taking $H = 1.0$, where the sharp peak at $m = 1$ can be observed. (b) and (c) show results obtained for $T = 0.8$ and $T = 1.0$, respectively. More details in the text.

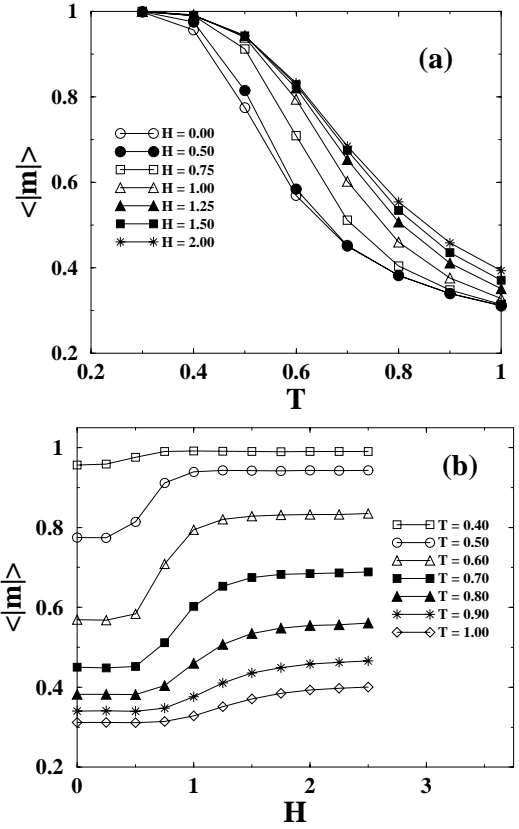


Fig. 2. (a) Plots of the order parameter versus the temperature obtained for different values of the surface magnetic field as indicated in the figure. (b) Isotherms showing the dependence of the order parameter with the surface magnetic field, obtained for the temperatures indicated in the figure.

the amount of disorder in the aggregate is large enough so that $P_L(m)$ becomes peaked around $m \gtrsim 0$ and the average magnetization is close to zero. The Gaussian-like shape of the distribution curves for $H < 0.5$ becomes distorted by the effect of the field causing a shift of the whole distribution towards larger values of m as well as the occurrence of a sharper peak at $m = 1$, that grows with increasing the applied field and becomes dominant for $H \geq 1$. For higher temperatures ($T = 1.0$ in Fig. 1c) the Gaussian shape for weak fields can clearly be observed, while the bias caused by the field has minor influence as compared with the former cases (Figs. 1a, b). Due to the observed fluctuations of $m(T, L, H)$, the order parameter as defined by equation (3) will tend to vanish upon averaging over all frozen columns. Therefore, in order to avoid this effect, it is convenient to redefine the order parameter as the average of the absolute column magnetization [9], *i.e.*

$$\langle |m(L, T, H)| \rangle = (1/M^*) \sum_{i=1}^{M^*} |m(i, L, T, H)|, \quad (4)$$

where $M^* < M$ is the number of frozen columns where the growing process has definitively stopped, that is, the number of completely filled columns. Figure 2a

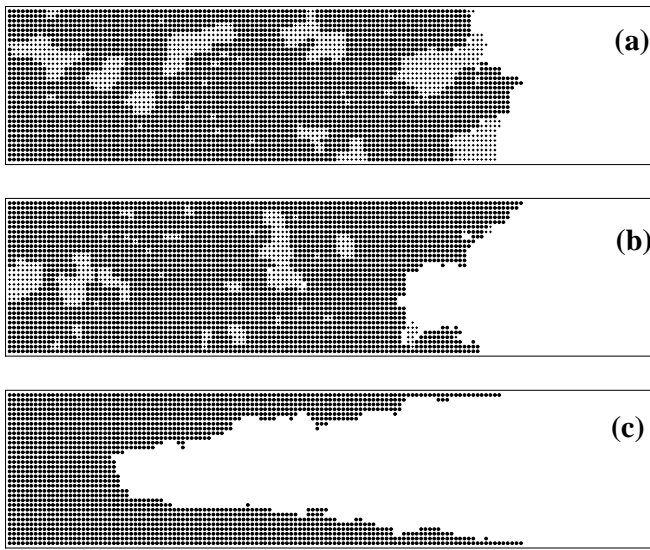


Fig. 3. Snapshot showing typical configurations of magnetic Eden aggregates. Filled circles and crosses correspond to spins pointing up (parallel to the magnetic surface field) and spins pointing down, respectively. The lattice width is $L = 32$. (a) $T = 0.67$ and $H = 0.0$. (b) $T = 0.67$ and $H = 1.33$. (c) $T = 0.33$ and $H = 1.33$.

shows the dependence of $\langle |m(L, T, H)| \rangle$ on the temperature for different values of the field, while Figure 2b shows the plots of $\langle |m(L, T, H)| \rangle$ versus H obtained at different fixed temperatures. At low temperatures (say $T < 0.4$) and even for very weak surface fields, the growth of magnetic Eden aggregates with chiefly parallel-oriented spins is observed. The absolute magnetization (and consequently the order) also remains quite large even when temperature is increased up to $T = 1$ (Fig. 2a). When comparing these plots with standard magnetic systems in equilibrium, *e.g.* the Ising model with surface fields [9], it is clear that for the lattices used in this work the MEM order-disorder transition is strongly rounded due to finite-size effects. The isotherms of Figure 2b show that for each studied temperature there exists a surface magnetic field capable of causing the saturation of $\langle |m| \rangle$. Of course, the dependence of the order parameter on the surface field at fixed temperature is smooth, in contrast with the jumps observed in the Ising system. This is not only attributable to finite-size effects. Actually, the fact that the magnetic fields are only applied to the boundaries of the aggregate (but not to the whole bulk of spins) plays a major role.

Figure 3 shows typical MEM snapshot configurations obtained at different temperatures and surface fields. The different shapes of the growing interfaces observed in Figure 3 can be understood on the base of simple arguments. For $H = 0$ and due to the fact that open boundary conditions are imposed at $j = 1$ and $j = L$, empty perimeter sites at the walls of the sample will experience a mixing neighbor effect, that is, the average number of NN occupied sites will be lower than for the case of perimeter sites on the bulk. Consequently, the system will preferentially grow along the center of the sample as compared

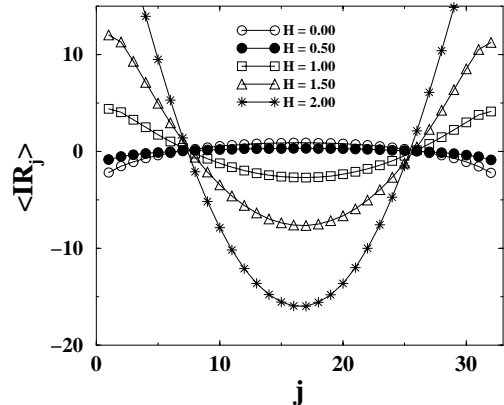


Fig. 4. Plots of the averaged interface profile versus j obtained for $T = 0.7$ and different values of the surface magnetic field as indicated in the figure. The plot corresponding to $H = 2.0$ has been truncated in order to allow a detailed observation of the profile's curvature for lower H values.

to the walls, and the resulting growth interface will exhibit a convex shape (Fig. 3a). For $H > 0$, the growing probability of perimeter sites at the walls of the system will be favored by an additional probabilistic factor given by $\exp(\pm H/T)$, as it follows from equation (2). If H/T becomes large enough, the preferential growth along the walls will dominate (Figs. 3b and 3c) and the interface curvature will become concave. So, from a qualitative point of view, the Figures 3a, b, c allow us to expect the occurrence of a convex-concave transition in the curvature of the growth interface. Such transition is identified as a non-equilibrium magnetic wetting transition, since a concave interface wets the walls while they remain dry when the interface grows with convex curvature.

In order to perform a quantitative study of the wetting transition it is convenient to define the location and the curvature of the growing interface. We assume that each row of the system contributes with the outermost perimeter site (*i.e.*, the one with the largest value of the longitudinal i th coordinate, for a given row number j) to the growing interface. Let $I_j(t)$ be the i th abscissa corresponding to the j th row at time t . Then, the interface center of mass, that we take as the location of the interface at time t , $I(t)$, is given by

$$I(t) = (1/L) \sum_{j=1}^L I_j(t). \quad (5)$$

Subsequently one can evaluate the coordinates of the interface relative to its center of mass location at time t , namely $IR_j(t) = I_j(t) - I(t)$, $j = 1, 2, \dots, L$. In this way we obtain a set $\{IR_j(t)\}$ that appropriately describes the interface at any time t during the growing process. In order to increase the statistics, we may evaluate the average relative interface $\langle IR_j \rangle$ given by

$$\langle IR_j \rangle = \{1/(t_f - t_i + 1)\} \sum_{t=t_i}^{t_f} IR_j(t) \quad (6)$$

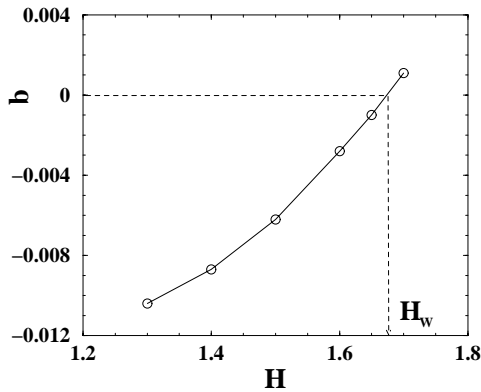


Fig. 5. Plot of b versus H obtained for $T = 2.00$. The dotted line shows the point where b changes its sign allowing us to identify the critical wetting field (H_w), as indicated in the figure. More details in the text.

where we take into account interface coordinates measured at different times between t_i and t_f . Figure 4 shows plots of $\langle IR_j \rangle$ versus j corresponding to $T = 0.7$ for different values of the surface field H . There, it becomes evident how the applied field drives the convex-concave curvature change. The curved interfaces have been fitted by means of a fourth-degree polynomial given by $p(j) = a + bj^2 + cj^4$, where $a = (L+1)/2$. All fits were characterized by a dominant quadratic term which defined the interface curvature and a practically negligible quartic coefficient. Thus, the sign change of the quadratic coefficient b allows the identification of the convex-concave curvature transition: for $b > 0$ the interface is concave and the cluster wets the walls, while for $b < 0$ it is convex and the walls remain dry. So, given a fixed temperature T , the magnetic field at the wetting transition H_w is the one that corresponds to $b = 0$. Figure 5 shows a plot of b versus H obtained for $T = 2.0$, where the change of sign of b can clearly be observed. In this example, by means of a linear interpolation, the value $H_w = 1.67 \pm 0.03$ is obtained.

Following this procedure, we can quantitatively obtain the wetting phase diagram H_w versus T . These results are shown in Figure 6, which corresponds to strip widths $L = 32$ and $L = 64$. They also suggest that the location of the critical wet non-wet curve is only weakly sensitive to finite-size effects. The monotonic growth of the H_w versus T curves shown, reflects the fact that a larger surface magnetic field is needed in order to stabilize the thermal noise caused by higher temperatures.

4 Conclusions

In this work, rectangular strips on the square lattice are used to grow magnetic Eden clusters with ferromagnetic interactions between nearest neighbor spins and short range magnetic fields applied at the surfaces. For weak surface fields, the mixing neighbor effect at the surface causes the growth of convex interfaces. However, when the field is increased, the preferential growth of spins along the surface turns the interface curvature concave. Such curvature change has been rationalized in terms of a wetting transition, and the corresponding wet non-wet phase diagram

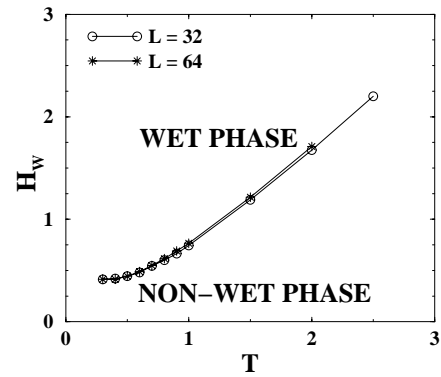


Fig. 6. Wetting phase diagram, H_w versus T , showing the critical line at the boundary between the wet and non-wet phases. Results obtained for $L = 32$ and $L = 64$, as indicated in the figure.

has been evaluated. We expect that the present study will stimulate further work in the field of non-equilibrium wetting transitions, a topic of widespread technological and scientific interest which has remained almost unexplored till the present.

This work is supported financially by CONICET, UNLP, CIC (Bs. As.), ANPCyT and Fundación Antorchas (Argentina) and the Volkswagen Foundation (Germany).

References

1. F. Family, T. Vicsek, *Dynamics of Fractal Surfaces* (World Scientific, Singapore, 1991).
2. A.L. Barabasi, H.E. Stanley, *Fractal Concepts in Surface Growth* (Cambridge University Press, New York, 1995).
3. *Fractals and Disordered Media*, edited by A. Bunde, S. Havlin (Springer-Verlag, Heidelberg, 1991).
4. *Fractals in Science*, edited by A. Bunde, S. Havlin (Springer-Verlag, Heidelberg, 1995).
5. M. Marsili, A. Maritan, F. Toigo, J.R. Banava, *Rev. Mod. Phys.* **68**, 963 (1996).
6. S. Dietrich, in *Phase Transitions and Critical Phenomena*, edited by C. Domb, J.L. Lebowitz (Academic Press, London, 1988), Vol. 12, p. 1.
7. A.O. Parry, *J. Phys. Cond. Matter* **7**, 10761 (1996).
8. H. Hinrichsen, R. Livi, D. Mukamel, A. Politi, *Phys. Rev. Lett.* **79**, 2710 (1997).
9. E.V. Albano, K. Binder, D. Heermann, W. Paul, *Surf. Sci.* **223**, 151 (1989).
10. M. Eden, in *Symp. on Information Theory in Biology*, edited by H.P. Yockey (Pergamon Press, New York, 1958); *Proceedings of the Fourth Berkeley Symposium on Mathematics, Statistics and Probability*, edited by F. Neyman (University of California Press, Berkeley 1961), Vol. IV, p. 223.
11. M. Ausloos, N. Vandewalle, R. Cloots, *Europhys. Lett.* **24**, 629 (1993); N. Vandewalle, M. Ausloos. *Phys. Rev. E.* **50**, R635 (1994).
12. J. Shen *et al.*, *Phys. Rev. B.* **56**, 2340 (1997).
13. U. Bovensiepen *et al.*, *Phys. Rev. Lett.* **81**, 2368 (1998).
14. E.V. Albano, K. Binder, W. Paul, *J. Phys. A* **30**, 3285 (1997).
15. K. Binder, *Z. Phys. B* **43**, 119 (1981).